Journal of Manufacturing Processes 124 (2024) 1259–1272

Contents lists available at ScienceDirect

Journal of Manufacturing Processes

journal homepage: www.elsevier.com/locate/manpro

Characterization of friction coefficient at near solidus forming (NSF) conditions using T-shape compression test

Muhammad Sajjad [a,*], Julen Agirre [a], Gorka Plata [a], Jokin Lozares [b], Joseba Mendiguren [a]

[a] Mondragon Unibertsitatea, Faculty of Engineering, Mechanics and Industrial Production, Loramendi 4, Mondragon 20500, Gipuzkoa, Spain
[b] Department of Mechanics, Design and Industrial Management, University of Deusto, Avda. Of Universities 24, 48007 Bilbao, Spain

ARTICLE INFO

Keywords:
Near solidus forming (NSF)
Finite element model (FEM)
Geometric parameter indexes (GPI)
Inverse modelling

ABSTRACT

Amidst the escalating demand for sustainable manufacturing practices aimed at mitigating global emissions and waste, industries are actively seeking novel forming solutions to address these pressing global challenges. Near Solidus Forming (NSF) processes emerge as a promising alternative to confront such issues, offering the capability to fabricate intricate components reliably while minimizing material waste and energy consumption. This promising manufacturing process is still in its developmental stages for industrial applications, necessitating further exploration and understanding of various factors such as friction, heat transfer, and others. From the literature review, a lack of friction data at these temperatures has been identified. Therefore, this study is dedicated to the advanced characterization of the friction coefficient for Near Solidus Forging (NSF) operations. With that aim, T-shape experimental tests of 42CrMo4 alloy steel have been conducted at high temperatures (up to 1360 °C). Additionally, a lack of consensus on the correct T-shape testing and inverse analysis procedure has been noted. Consequently, apart from the experimental work, an in-depth analysis of the friction coefficient identification procedure has been conducted. As a result, a new geometrical output index is proposed, highly sensitive to the friction coefficient and therefore more reliable compared to state-of-the-art indexes. Furthermore, the influence of the selected geometrical output index and the consideration of sample-to-sample transfer and holding times were studied. Results showed that the increase in workload to consider the sample-to-sample transfer and holding times is not worthwhile, as assuming the average values lead to significantly less work with little impact in the final results (<5 % of error). The study also concludes that a friction coefficient of 0.25, 0.45 and 0.6 has been identified at temperatures of 1250 °C, 1300 °C and 1360 °C, respectively. Additionally, the result of thermal camera showed good agreement with the thermocouple data. Overall, in this study a robust and reliable T-shape testing, and friction coefficient identification procedure is proposed and validated.

1. Introduction

Forging at the semi-solid or near-solidus material state, known as Near Solidus Forging (NSF), is conducted at a temperature just below the liquidus point of a forming material. This process leverages the high ductility of the material in its soft-solid state while retaining most of the mechanical properties of a forged part. NSF has emerged as a promising technology with significant advantages over traditional forging processes. The process is capable of manufacturing complex parts with close to net shape, while reducing the amount of material waste and energy consumption [1,2]. However, the deformation behaviour of materials at such high temperatures is complex, often requiring a trial-and-error approach to achieve a desirable component. Therefore, despite the promising potential of the technology, the process lacks detailed investigation, thus generating doubt on the reliability of the numerical models employed in the finite element model (FEM) simulations of NSF. To ensure the accuracy of such model, the characterization of the major factors such as material, heat transfer coefficient and friction coefficient is necessary. According to the work of Sajjad et al., the friction coefficient (FC) has significant influence on both force and material behaviour during the NSF process [3]. Friction plays a pivotal role in determining the efficiency, quality, and cost-effectiveness of manufacturing operations, particularly at high temperatures where materials are more sensitive to temperature and other boundary conditions [4].

* Corresponding author.
E-mail addresses: msajjad@mondragon.edu (M. Sajjad), jagirreb@mondragon.edu (J. Agirre), gplata@mondragon.edu (G. Plata), jokin.lozares@deusto.es (J. Lozares), jmendiguren@mondragon.edu (J. Mendiguren).

https://doi.org/10.1016/j.jmapro.2024.07.009
Received 25 March 2024; Received in revised form 21 June 2024; Accepted 2 July 2024
Available online 10 July 2024

Therefore, a precise understanding and control of the friction coefficient are crucial as it directly impacts various aspects of the process. Firstly, it affects the material flow, as it influences the forming force required and ultimately determining the shape and dimensions of the final product [5]. Secondly, it significantly impacts the wear and tear on the forming dies, affecting their longevity and maintenance costs [6]. Additionally, the friction coefficient influences the energy consumption during the forming process, with higher friction leading to increased energy requirements. Moreover, it affects the surface finish and integrity of the formed parts, as excessive friction can result in defects such as cracks or surface imperfections [7]. Consequently, optimizing the friction coefficient is essential for enhancing productivity, reducing costs, and ensuring the quality and integrity of the formed components.

To investigate the friction behaviour in various forming operations, friction characterization tests are performed. These tests replicate the contact conditions as closely as possible to hose encountered in the actual forming process [8]. This is essential because friction in forming processes is greatly influenced by factors such as pressure, surface contact, temperature, and lubrication conditions. Therefore, an effective friction testing method for individual forming processes should be implemented to ensure that the testing conditions closely mirror the real industrial scenarios, allowing for a more accurate assessment of frictional behaviour during forming [9]. Numerous techniques have been proposed in the literature, including ring compression, double-cup extrusion, spike forging tests, and T-shape compression tests. Mendiguren et al. used the ring compression test to characterize the friction coefficient of AISI 304 L at hot forging conditions while Galdos et al. carried out double-cup extrusion test to evaluate the impact of the lubrication layer in Ti64 forging [10,11]. Furthermore, Jeong et al. used the spike forging test for the evaluation of friction coefficient at both dry and lubricant conditions while Sethy et al. proposed the T-shape test for the identification of friction coefficient in aluminium alloy at high temperatures [12,13].

Multiple studies demonstrated that the ring compression test is widely used due to its simple setup and ease of determining the shear friction factor (m) or the friction coefficient (FC), which was initially developed by Male and Cockcroft in 1964 [14]. The test involves compressing of a flat ring specimen, with the change in internal diameter reflecting the friction level. However, it is important to note that this test induces a relatively uncomplicated deformation path and a relatively small surface expansion ratio, therefore, makes it less suitable for processes with significant surface expansion. Research by Jeong et al. (2011) suggests its application should be limited to friction factors below 0.3 [15].

Initially proposed by Buschhausen et al. in 1992, the double cup extrusion method was further developed by Arentoft et al. in 1996 [16,17]. The setup for double cup extrusion comprises four main components: upper punch, lower punch, container, and specimen. During the process, the upper punch moves downward with the press ram while the lower punch and container remain stationary. Due to the relative velocity between the container and the upper punch, friction along the container's surface can cause relative metal flow into the upper cup compared to the lower one. Consequently, the ratio of the height of the top cup to that of the bottom cup is dependent upon the friction along the container. The cup height ratio increases with greater friction along the container/specimen interface. If no friction force is generated along the inner surface of the container, the minimum cup height ratio is estimated equals to one. However, Schrader et al. (2007) observed that the maximum contact pressure between the specimen and the container is relatively low (e.g., <700 MPa in his study for low-carbon steel) [18]. Additionally, Arentoft et al. (1996) discovered that the strain hardening rate of the material significantly influences the cup height ratio and the assessment of the friction coefficient [17]. While the double-cup extrusion test, as highlighted by Buschhausen et al. (1992), provides a more accurate friction factor by preserving lubricant in the die-workpiece interface, Schrader et al. (2007) found its friction factor estimation relatively small due to lower contact pressure.

Spike test represents an axisymmetric forging technique that integrates extrusion and upsetting processes. First demonstrated by Xu and Rao (1997), the test is suitable for evaluating friction in complex deformation processes [19]. It serves as a viable method for evaluating friction since both the load and spike height increase with friction. The spike forging test consist of a bottom die featuring a sharp-cornered tapered shape of circular cross-section, along with a flat-top die [20]. During the process, a circular billet compressed between these dies undergoes both lateral and orifice-directed flow. Higher friction resists the lateral flow, resulting in a longer spike extrusion [21]. Similar to the ring compression test, in this setup, the ends of the cylindrical specimen come into direct contact with the die and punch. However, this test exhibits the smallest contact pressure and surface expansion ratio among the presented methods.

Zhang et al. (2009) proposed the T-shape compression test to mitigate friction variations on round billet surfaces, achieving a surface expansion ratio of 24 % and contact pressure up to 2.5 times the flow stress [8]. This method has been used by Fereshteh et al. to assess the friction factor of magnesium alloys at elevated temperatures with promising outcomes [21]. The T-shape compression test stands out as an ideal choice for closed die high-temperature forming processes for several reasons. Firstly, this method allows for the evaluation of friction under conditions closely resembling those encountered in industrial processes [22]. By positioning the round billet horizontally, only the cylinder surface comes into direct contact with the dies, reducing variations in friction conditions between different surfaces. Secondly, the T-shape compression test facilitates a significant surface expansion ratio, reaching up to 24 %, providing a more realistic representation of the deformation encountered in high-temperature forming processes. Additionally, the contact pressure achieved in this test can be substantially higher, up to 2.5 times over the flow stress, enabling a more accurate assessment of frictional behaviour under high-temperature conditions. Consequently, the T-shape compression test offers a reliable means of evaluating friction in closed die high-temperature forming processes, contributing to improved process optimization and product quality.

The influence of transfer and holding times on the deformation behaviour of hot forged steel components has been investigated in several studies. Yan et al. examined the effects of forming temperature, soaking time, and dwell time on the microstructure and mechanical properties of the formed parts. The authors discovered a significant change in material behaviour when these parameters were altered [23]. Another study by Rooks et al. focused on the hot deformation behaviour of 1000 steel billets using flat dies. He concluded that a change in dwell time from 5 ms to 1 s had a noticeable effect on material behaviour during forging [24]. Additionally, a study demonstrated the effect of the holding time on the plastic forming of Ti-6Al-4 V micro-gears at elevated temperatures, showing similar results [25]. These findings highlight the importance of transfer and holding times in determining the deformation behaviour of hot forged steel components. However, the conventional approach to T-shape compression testing typically involves conducting multiple repetitions and employing a single averaged transfer and dwell time for inverse engineering analysis [13].

Several studies have investigated the selection of the correct parameter output index for the characterization of the friction coefficient, which can lead to different results depending on the testing material and temperatures. Zhang et al. employed the height of the extruded T-shape part for the evaluation of friction coefficient by comparing the experiment data with the simulation [8]. Similarly, Deng et al. used the same method but rather than using the extruded height as principal index they combined the extruded height with the width to

conclude his friction coefficient analysis [9]. Furthermore, Galdos et al. recently considered other geometric index such as total width and flange height for the characterization of friction in titanium Ti64 alloy [11]. These findings highlight the importance of selecting the most suitable geometric parameter index (GPI) for the individual material and process conditions.

Interestingly, numerous studies have been conducted on the T-shape test for various forming process at elevated temperatures. Barati et al. employed the T-shape test to characterize the friction in Ti-6Al-4 V alloy at elevated temperatures while Ben et al. proposed the same method for the analysis of friction behaviour in the oscillating forming process, same methods were used by other authors such as Barati et al., Yoon et al., for the identification of friction at high temperatures [26,27].

From the literature it is clear that the friction coefficient plays a pivotal role in the development of reliable material models. Liu et al. proved that the friction coefficient significantly influences the heat input and material flow characteristics in the process which is vital factor in process modelling [28]. Other authors concluded the same remarks such as Meyghani and Dialami et al. in the characterization of friction stir welding process at elevated temperatures [29,30]. Moreover, friction data in the forming process, specifically under NSF conditions where the material is formed close to its solidus state is limited [1]. Due to the complex behaviour of the material at the NSF conditions, there exists a significant lack of data in the literature regarding friction coefficient characterization. Furthermore, the transfer and holding time in the T-shape test is typically neglected at hot forming conditions. However, in the NSF where the temperature loss have a great impact on the process the characterization of these factor is necessary [31]. Lastly, the sensitivity of the GPI introduced in the T-shape test, such as total height, total width, and flange height is not studied previously in the NSF process, therefore, necessitate its investigation for the accurate characterization of the friction coefficient at these conditions.

To the best of the authors' knowledge, three primary research gaps have been identified in the characterization of friction coefficient (FC) for Near Solidus Forging (NSF): ① No literature has been found on FC characterization at NSF temperatures; ② there is no consensus in the community regarding the optimal geometrical parameter index (GPI) for the FC characterization employing T-shape tests, particularly at NSF temperatures; and ③ despite the critical importance of transfer time and dwell time in hot forging, no studies have been found that evaluate the cost-benefit of using exact values for each repetition compared to averaged values for T-shape FC characterization.

To address these gaps, this study aims to characterize the FC at NSF conditions by employing the T-shape compression test. The T-shape test was conducted at three temperatures: 1250 °C, 1300 °C, and 1360 °C. Following the tests, GPI like total width and flange height were measured for subsequent FC characterization. A three-dimensional finite element model of 42CrMo4 steel for the T-shape compression test was constructed utilizing the FORGE NxT® 4.0 FEM software. Inverse modelling techniques were employed to conduct simulations at six varying FC values ranging from 0.01 to 1.0. Based on the literature, the evolution of flange height and total width was continuously monitored and compared to experimental results to determine the FC value. However, while using this approach, the typical total width and flange height introduced uncertainties, hence command the development of a new approach for accurate FC characterization. For this purpose, a new parameter has been introduced which is more sensitive to friction and temperature: the ear width. Furthermore, the influence of transfer and holding time has been studied based on the experimental data.

2. Research methodology

2.1. Tested sample and description of the T-shape testing facility

The tested sample were cut from a rod of 42CrMo4 steel by wire electrical discharge machining (EDM), resulting in a cylindrical geometry with a diameter of 20 mm and a height of 20 mm, with a machining tolerance of ±0.1 mm, as depicted in Fig. 1(a). The forging tools were made from Uddeholm Alvar 14 tool steel (1.2714/EN 56NiCrMoV7). To achieve the desired "T" shape profile in the test, the lower die was machined with a V-shaped groove through wire EDM and then hardened to a level of 42 HRC. Surface roughness of test-tooling systems is around 2.70 µm. The groove had a 15° angle β, a 2.5 mm entry radius, a total depth of 25 mm, and a final radius of 1 mm, following the work of Sethy et al. [13]. The detailed dimensions of the groove and T-shape tooling are shown in Fig. 1(b). The T-shape die was mounted in a tool-holder to fix its movement during the testing.

In this investigation, the tests were performed in a high-precision 400 t FAGOR SDM2–400–2400-1200 servo motor-operated mechanical press, as illustrated in Fig. 2. The press was programmed to achieve a flange height, or press gap, of 4.5 mm during the test, which is 85 % of the total height typically used in the T-shape compression test. The characteristics of the press are detailed in Table 1. To minimize the heat transfer from the billet to the dies, the dies were heated to a temperature of 170 °C employing a set of 630-watt Hasco cartridge die heaters, which were connected to the main T-shape die-set, labelled 6 in Fig. 2. Furthermore, it ensured a precise temperature control during the tests. Two thermocouples were strategically positioned between the dies and the digital temperature control box (labelled as 1 in Fig. 2) in order to effectively regulate the dies' temperature. Before initiating the tests, a CeraSpray® lubricant was applied using a pistol-spray onto both the upper and lower dies, in order to minimize friction and heat loss to the dies, replicating the industrial NSF procedure [1]. During testing, the forming forces were measured using a 500 tons load cell.

The kinematics of the mechanical press were acquired by an optical displacement sensor (Leuze Electronic ODSL 8/V66–200-S12), labelled 3 in Fig. 2. A thermal camera was also employed to acquire the sample temperature profile during the tests, labelled 2 in Fig. 2. To ensure the robustness of the obtained results, three repetitions were carried out per tested condition.

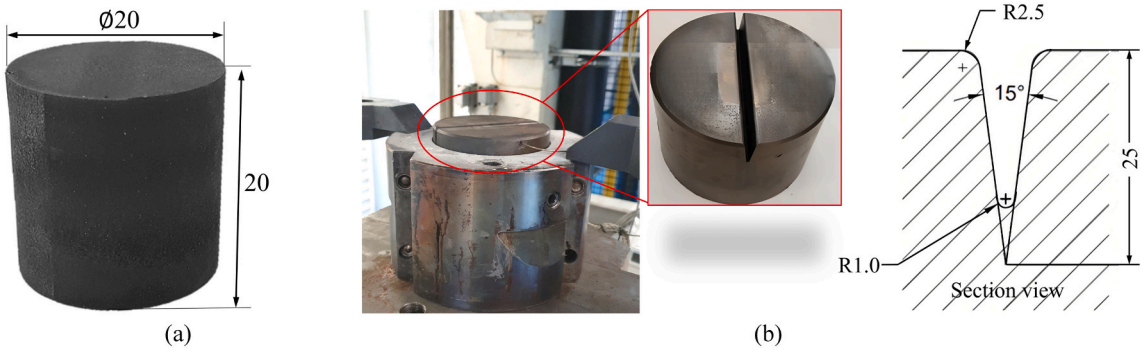

Fig. 1. a) T-shape test sample, b) (left) experimental grooved die, (right) the sectional view of the die.

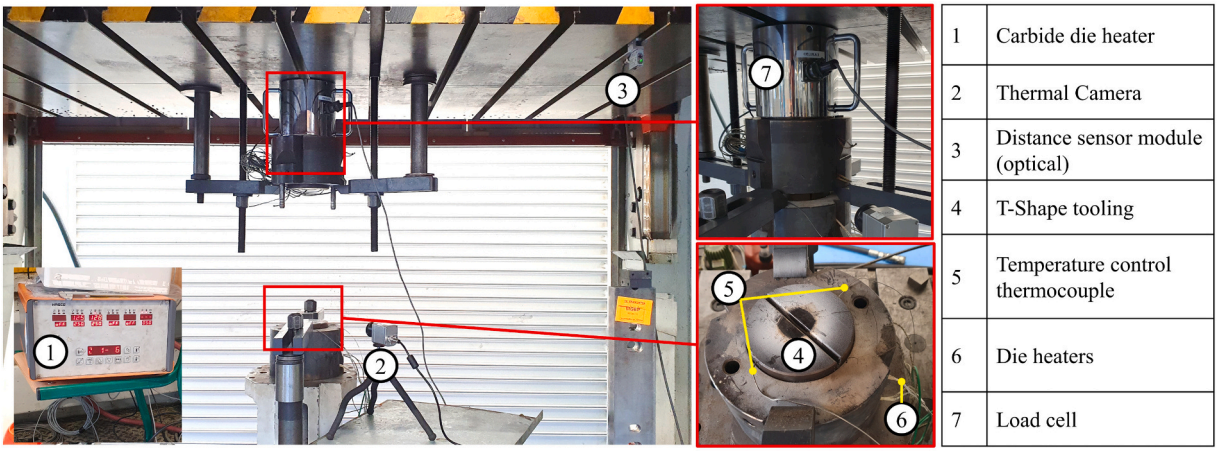

Fig. 2. Detailed view of T-shape test equipment.

Table 1
Boundary conditions of the T-Shape compression test.

Billet temperature (°C)	Die temperature (°C)	Ambient temperature (°C)	Lubricant Type	Material
1250 1300 1360	175	20	CeraSpray®	42CrMo4 steel

2.2. Test procedure

The temperature range selected for this test was considered based on the Near Solidus Forging (NSF) conditions for 42CrMo4 steel, as utilized by other authors in their studies [2,32]. In this study, the experiments were conducted at three temperatures: 1250 °C, 1300 °C, and 1360 °C. The specimens were heated to the desired temperature in a Hobersal CRN-5×/17 electrical furnace and held at the testing temperature for five minutes for temperature homogenization. After the holding time, the specimen was handled to the testing position with an average transfer time of three seconds. The specimen was compressed between the dies after a holding time of two seconds. The testing procedure can be seen in Fig. 3(a). The press movement was divided into three main stages: first, the press started its movement from the top dead centre towards the billet with high velocity; second, the deformation took place, where the deformation speed was recorded at around 17 mm/s; and finally, the press moved back to its starting position for the next test. The temperature profile of the test at 1250 °C is superposed on the same figure. The specimen before and after the test can be seen in Fig. 3(b). The testing conditions of T-shape compression tests are summarized in Table 1.

The cylindrical specimens were compressed between the T-shape tooling forming a T-shaped profile as shown in Fig. 4(a). After the tests, various GPI were measured for the inverse analysis. These variables are presented in Fig. 4(b), which include the total height (H), the total width (w), the delta height (ΔH), the delta width (Δw), and the flange height (h). These variables are vastly used for the characterization of friction coefficient in the T-shape test for various metals. The measured dimensions of the variables in the tested specimen can be seen in Fig. 4(c). All the measurements were conducted through a digital vernier calliper.

2.3. Numerical analysis

The friction coefficient identification through T-shape testing involves an inverse engineering step, wherein the friction coefficient is iteratively adjusted numerically until the numerical geometrical parameter index (GPI) fits the experimental GPI. In this context, a 3D finite element model of 42CrMo4 steel for the T-shape compression process was developed in the FORGE NxT® 4.0 finite element software, as shown in the Fig. 5. Fig. 5(a) represents the initial stage of the process while (b) shows the deformed sample. The employed software is capable of numerically simulating large strain thermo-plasticity, contact and friction boundary conditions. The visco-plastic behaviour of the material was modelled with the Hansel–Spittel hardening model, which

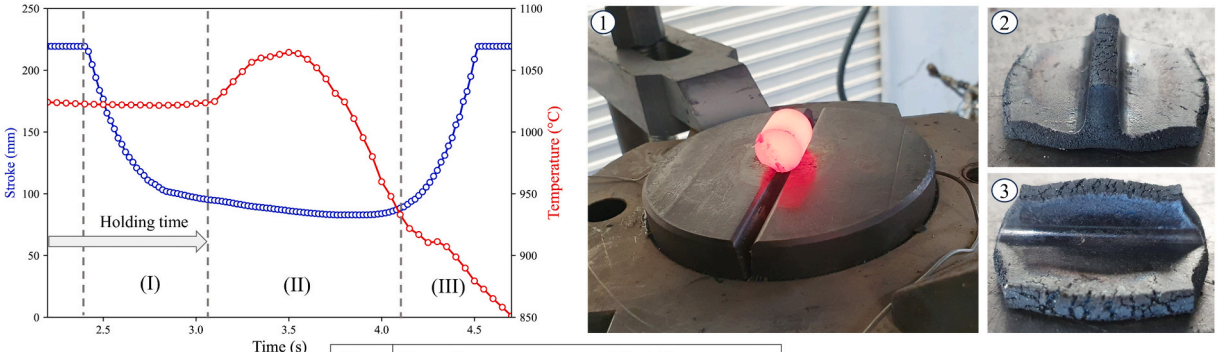

(I)	Press die movement toward the billet
(II)	Deformation phase of the billet
(III)	Die movement toward the Top Dead Centre

Fig. 3. T-shape testing: a) punch configuration and its phases, b) deformed test samples; (1) pre-formed, (2,3) post-formed.

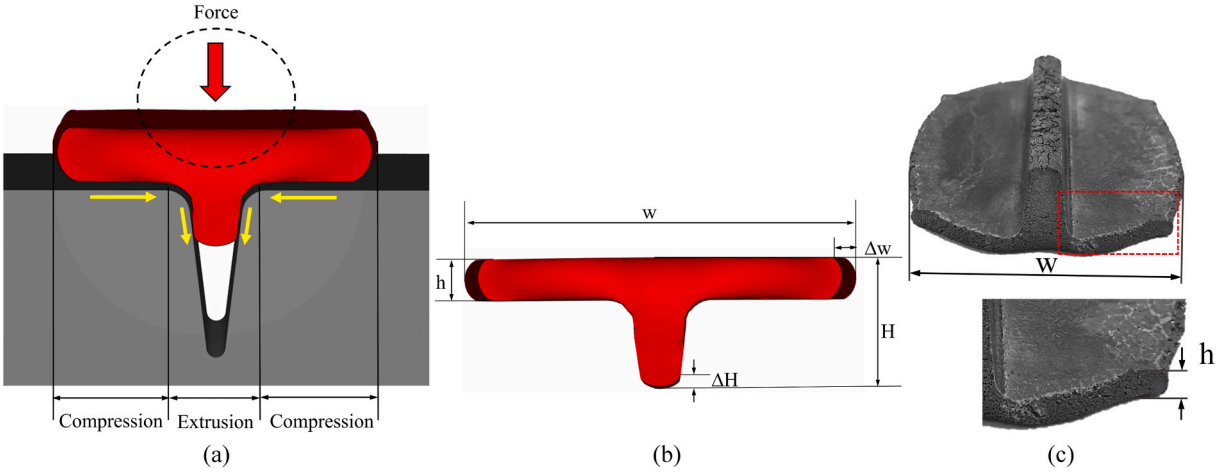

Fig. 4. T-shape testing and GPI definition: a) deformation characteristics of the sample, b) sample dimensions, and c) height and width measurements.

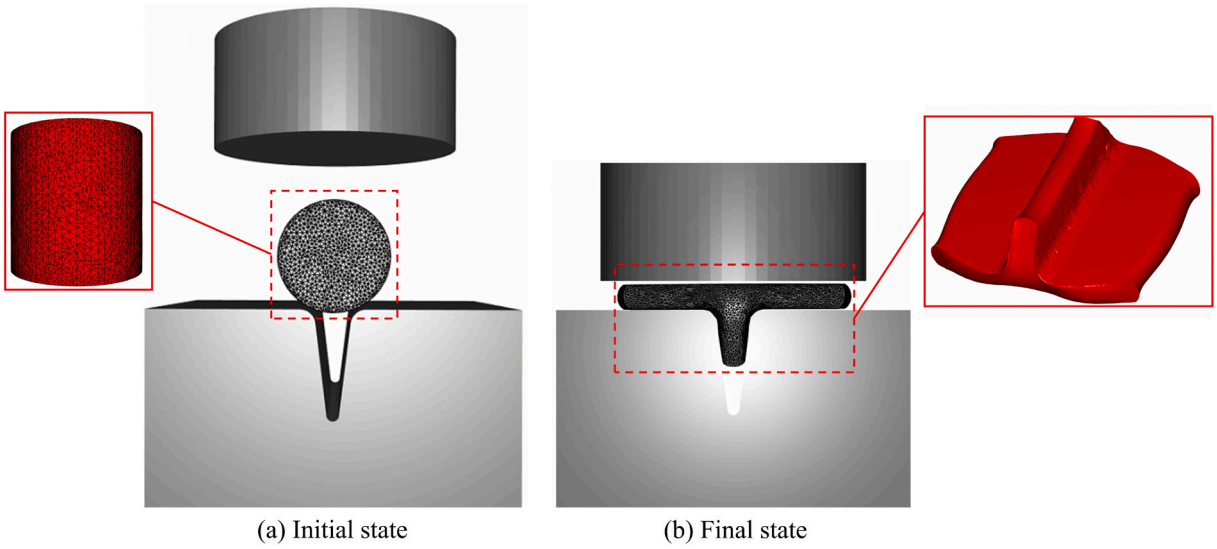

Fig. 5. Specimen deformation process in FEM simulation: a) initial stage, b) final stage.

calculates the flow stress in function of the strain, strain rate and deformation temperature [3]. In the simulation the upper and lower tools were represented as rigid entities, with the unilateral contact and the heat transfer coefficient prescribed at the part/die interface. Furthermore, the contact was modelled by a Coulomb limited Tresca model implemented from the FORGE database. Based on the previous simulation work of the NSF process the heat transfer of 800 W/m^{2}K was established between the part/dies interface [2]. Moreover, the lower die remained stationary while a vertical displacement acquired experimentally was imposed on the upper die, details shown in Fig. 3(a). In the simulation, the dies were assigned a temperature of 170 °C, with the ambient set at room temperature (20 °C). The element type of the model is first order tetrahedron and the average mesh size employed in the billet was 0.5 mm with the minimum value of 0.05 mm. A remeshing strategy was employed to minimize the computational time and increase the accuracy of the simulation results. As a result, the number of elements is increased from 87,327 to 763,150, due to the remeshing rule at the end of the deformation phase. This numerical model corresponds to the standard used in previous studies in the literature such as NSF of automotive components [32] and thixoforging of low carbon steel tubes at a flashless forging process [33].

To include the initial temperature distribution prior to the deformation stage, the simulation process is partitioned in three main stages. In the first stage, the sample cooling is simulated during the billet transfer from the furnace to the testing position, while employing the exchange of heat with air along the billet's entire boundary surface. Next, in the second stage the temperature evolution is simulated for the pre-compression holding time, when the billet was placed on the lower tool. Finally, the upper tool was subjected to a predefined kinematics, explained in the Fig. 3(a) and the deformation took place. It is worth to mention that the simulations were conducted employing various friction coefficient: 0.01, 0.1, 0.2, 0.4, 0.6, 0.8, and 1.0. And the evolution of different GPI were continuously monitored by virtual sensors and compared with experimental results to calibrate the exact friction coefficient.

Fig. 6 illustrates the detailed methodology employed in calculation the FC values, which consisted of three primary steps. First, the experimental phase which involved conducting the T-shape test and calculating the GPI such as the w/h ratio. Subsequently, in the second step, a numerical simulation of the process was conducted with different values of FC to generate geometric parameters index (GPI) curves, as depicted on the right-hand side of Fig. 6. Finally, the w/h ratio obtained from the experiment was plotted against the simulation curves. Based on the close correlation observed between the experimental data points and the simulation results, the optimal FC value was determined. If the point is directly located on the GPI curve, the exact value of FC will be

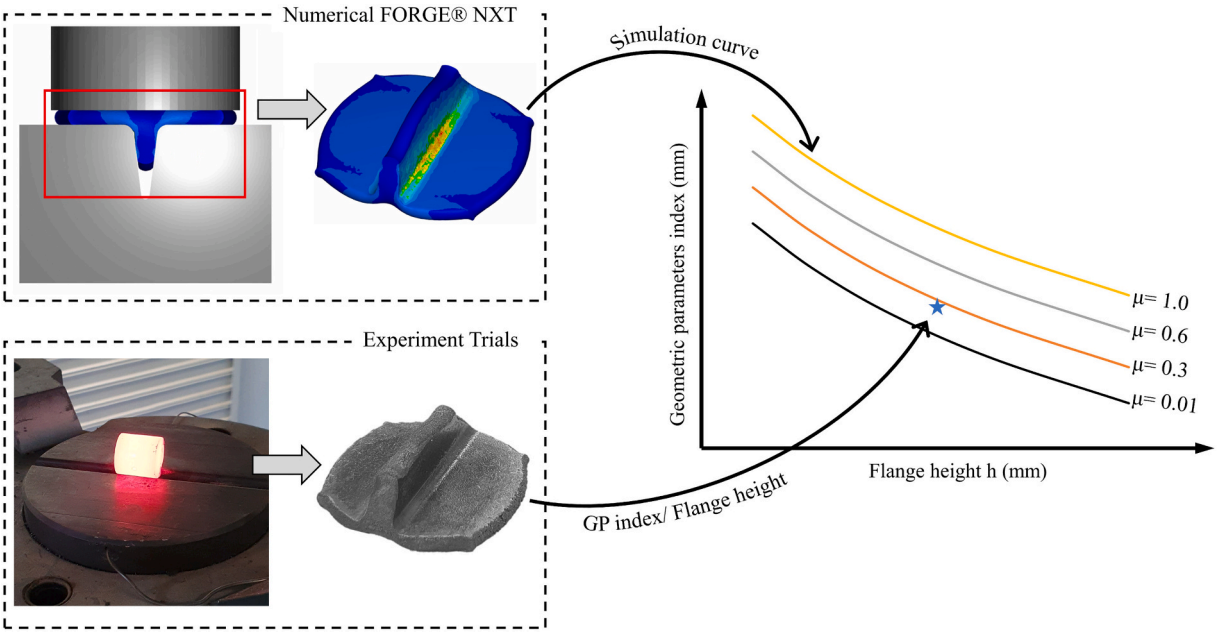

Fig. 6. Inverse analysis process flow chart.

considered, however if the experimental data point was located between two curves, then an estimate value between the range of both curves was calculated by linear interpolation.

Fig. 7 illustrates the samples from the T-shape test; the left side depicts the samples from the actual test, while the right side shows those from the simulations. A clear correlation between both sets of samples can be observed, as all the simulation samples. Moreover, at 1250 °C, it is evident that the simulation sample with a lower friction coefficient best represents the actual geometry of the test sample. Conversely, in the case of higher temperatures, the simulation sample with a higher FC accurately represents the test samples, suggesting an increase in FC value with the rise in temperature.

3. Results and discussion

As previously outlined, the T-shape compression test was conducted on 42CrMo4 steel samples at three temperatures to characterize the friction coefficient at NSF conditions. Fig. 8 presents the experimental forces observed at all temperatures (1250 °C, 1300 °C, and 1360 °C). The x-axis represents the upper die stroke, while the y-axis represents the corresponding forces. Each plot comprises three tests conducted under similar boundary conditions to assess the test's repeatability. Overall, the force curve behaviour exhibits satisfactory similarity across all test repetitions. A closer examination reveals that the forming forces are notably higher at 1250 °C, peaking at 19 t at the end of the process. This increase in force is attributed to the material temperature; the material at lower temperatures requires higher forces to deform and vice versa. Conversely, at 1300 °C, the tests demonstrate good repeatability. In the tests performed at 1300 °C, due to a higher sample temperature, the forces are comparatively lower than the previous tests, with peak forces noted around 16.5 t. Finally, at the highest temperature of 1360 °C, the peak force is registered around 15 tons, which shows further decline in the forming forces.

3.1. Geometric parametric index sensibility

Following the state-of-the-art review and gap definition of non-consensus on what is the ideal GPI, in this section the sensitivity of the total width and flange height is studied as principal index for this material and conditions. The total width (w) and flange height (h) of the

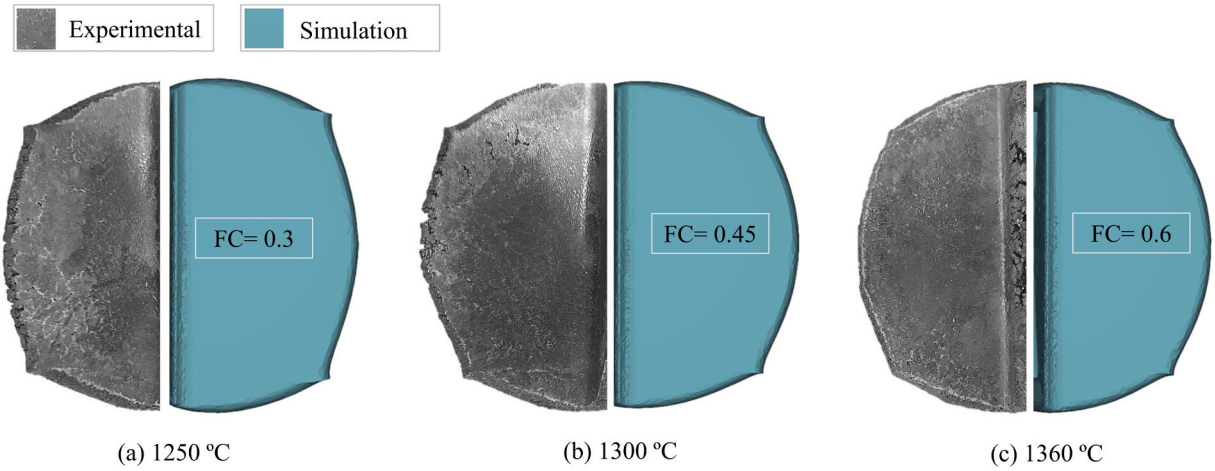

Fig. 7. Comparison of the deformed samples at all temperature (experimental vs simulation).

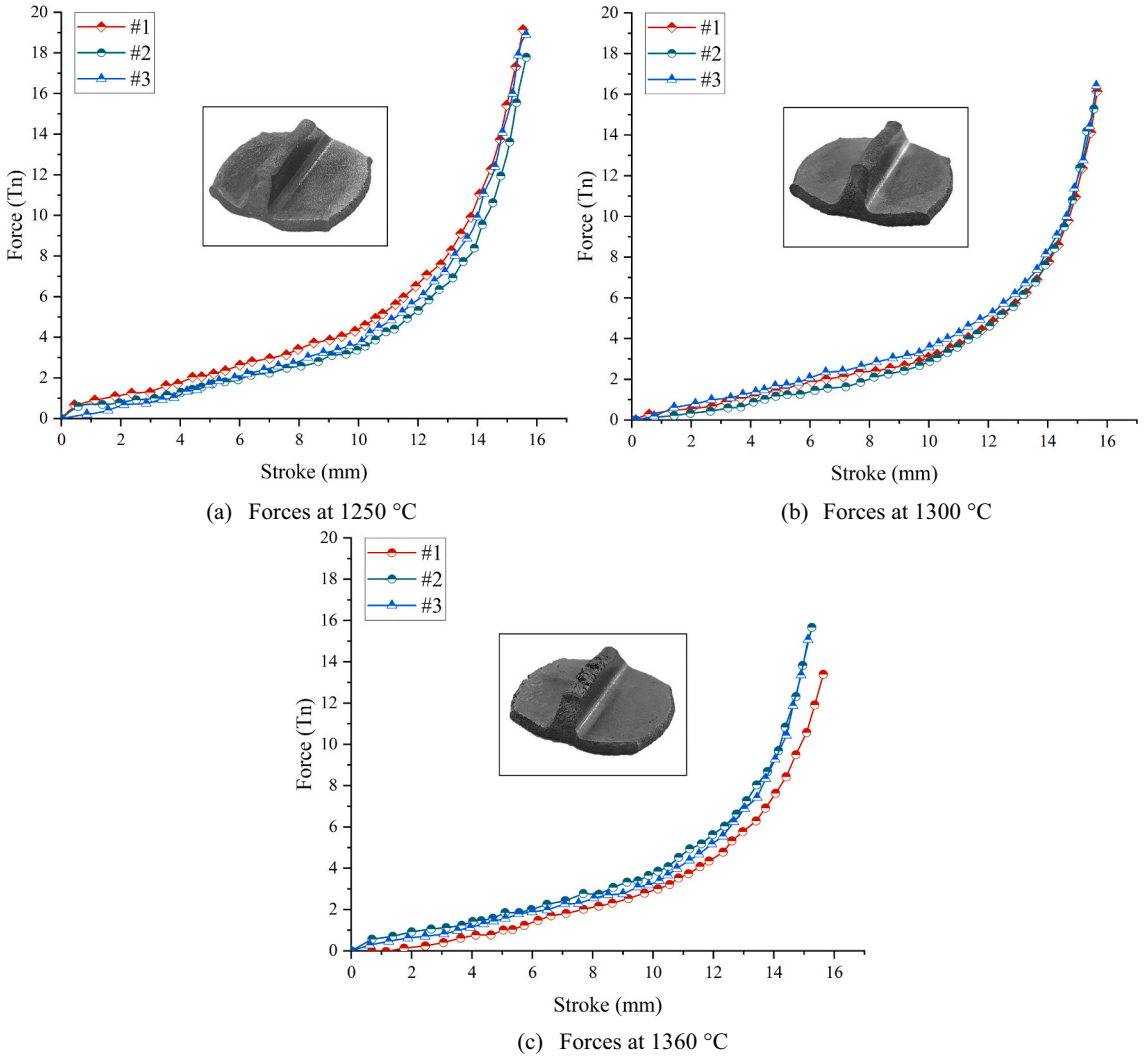

Fig. 8. Forces at three different temperatures (Experimental).

tested samples were computed. The parameter total width is specifically chosen due to their high sensitivity to the friction factor compared to other measurements, details of which can be found in the literature [8]. Following the T-shape test, the values of these two variables were measured, which are documented in Table 2. The results reveal the significant influence of the temperature on these two variables. At lower temperatures (1250 °C), a smaller value of w is observed. Transitioning to the next temperature (1300 °C), an increase in the material flow can be observed, resulting in a higher w value, averaging around 41.26 mm. Lastly, at the highest temperature (1360 °C), the maximum total width is noted, averaging at around 42 mm.

Table 2
Test results (total width and flange height).

Temperature (°C)	Test No.	Total width (w) [mm]	Flange height (h) [mm]
1250	#1	40.6	4.0
–	#2	41.9	3.8
–	#3	40.6	4.1
1300	#1	41.0	4.0
–	#2	41.7	3.8
–	#3	41.1	3.9
1360	#1	41.8	3.8
–	#2	42.0	3.6
–	#3	42.2	3.7

Theoretical considerations propose that as the friction factor increases, there is a sharp rise in the normal pressure. Consequently, the formation of extruded height ribs become more pronounced compared to lower values, thereby influencing the shape of the total width rib. Lower friction values result in a more uniform metal flow across the rib, manifesting nearly flat flowing front surfaces. As friction increases, the resistance encountered by the metal to flow in the horizontal filling direction also increases, leading to a more uniform metal flow pattern but shaping the flowing front surface into a distinct drum-like form (see Fig. 10(a)).

3.2. Determination of the friction coefficient

Using the flange height as the GPI the FC was calibrated using the previously explained methodology. Fig. 9 presents the measurements of the total width (w) evolution against flange height (h) for different friction factors obtained by numerical simulation and experimental trials at a temperature of 1250 °C. In this case the experimental tests were repeated three times (#1-#3) to provide different flange heights with different width in order to produce a data scatter from which a conclusion can be made. In the inverse modelling, various FC values (ranging from 0.01 to 1) were employed to calibrate the ratio of total width to flange height. Observing the figure, it is apparent that in the experimental trials, the ratio (w/h) highlights an area corresponding to a coefficient of friction around 0.15, which lies between the green line and

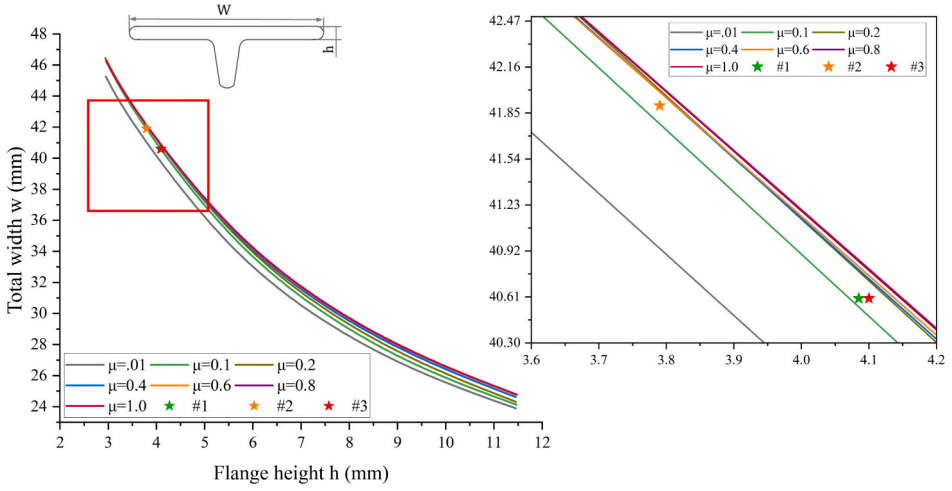

(a) 1250 °C

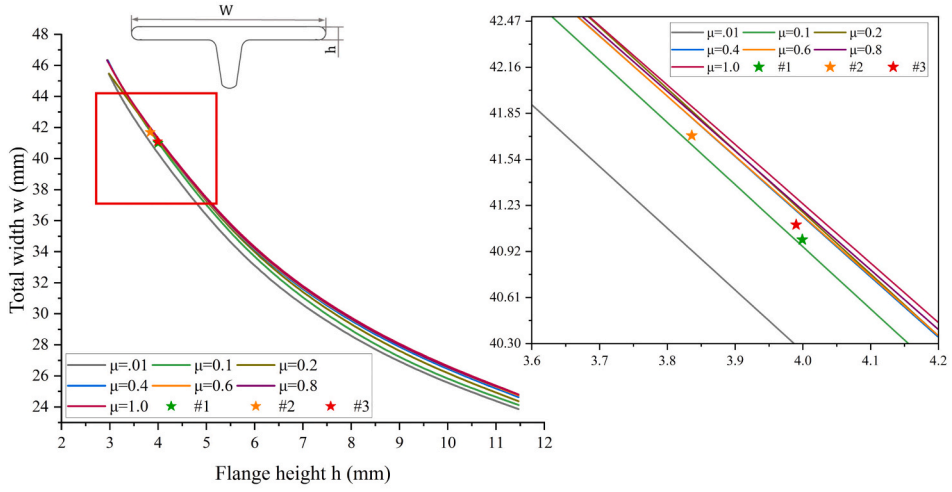

(b) 1300 °C

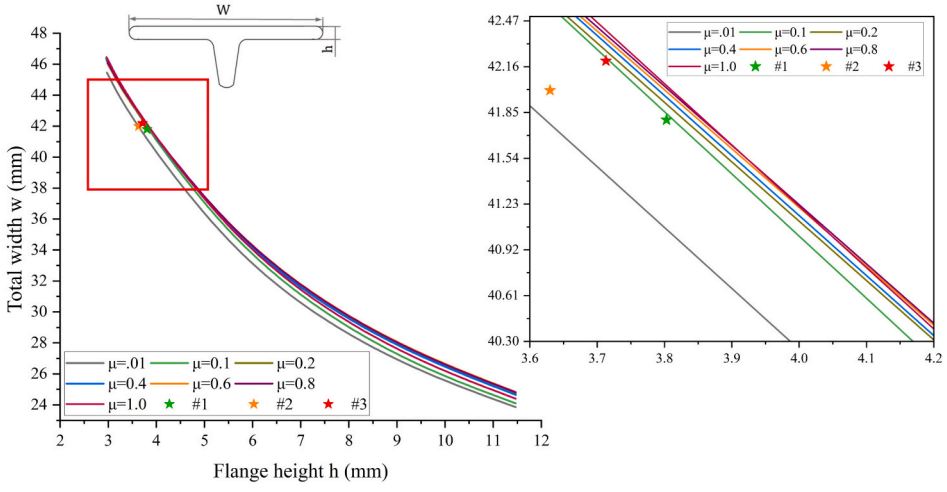

(c) 1360 °C

Fig. 9. Calibration curves of the T-shape test at 1250, 1300 and 1360 °C temperature.

the other plotted lines (see Fig. 9(a)). Although one test slightly deviates from the other two in terms of how much it was pressed, the overall results indicate that the final value of the friction coefficient at a temperature of 1250 °C averages around 0.15.

Similarly, at 1300 °C, a similar representation is depicted, with the plot revealing a correlation between the simulation and experimental values, as illustrated in Fig. 9(b). At 1300 °C, the (w/h) ratio lies again between the green and orange lines, a distinction clearly visible in the zoomed plot. The estimated value is calculated around 0.13 with a small difference in value from the previous temperature conditions. However, in the experiments one test diverges from the others (test = #3), possibly due to incorrect billet placement during testing. Nevertheless, a deeper

analysis of the data suggests that the coefficient of friction value at 1300 °C and 1250 °C are different by a small margin. Finally, at 1360 °C, a similar procedure for calculating the friction coefficient is employed, this time the experimental points fall between the grey and green lines, as depicted in Fig. 9(c). This indicates that the coefficient of friction at a temperature of 1360 °C is estimated to be around 0.08.

In summary, it is evident that there exists a minimal difference in GPI curve once the FC increase above 0.1 value, see Fig. 9. This suggests that the GPI employed so far may lack the necessary sensitivity for this material within the given temperature range. To further investigate this, a sensitivity analysis was conducted, examining the variation in GPI corresponding to temperature and FC, as illustrated in Fig. 10. Fig. 10(a) shows the results of parameter total width *w*. Firstly, the temperature exhibits a mixed influence on the *w* value. However, the most significant observation is the marginal difference in the *w* value due to an increase in the FC value, ranging from 38.75 mm to 40 mm, representing a total effective change of 1.25 mm. Similarly, Fig. 10(b) displays the results for the parameter *h*. Here, the effective difference attributed to the FC value is estimated to be around 2.25 mm, noticeably larger than that observed for the parameter *w*. Nevertheless, this small change in values could introduce uncertainty in the calculation of accurate FC value.

3.3. Development of a new approach

As concluded in the previous section, the GPI previously considered demonstrate minimal sensitivity to both temperature and FC values, indicating uncertainty in the accuracy of the proposed method. To address this challenge, a novel GPI is proposed, introducing a new geometric parameter index termed "ear width" (w_e), as depicted in Fig. 11(b). In this approach, the distance between two ears on opposite sides of the T-shape geometry is taken into account for the FC characterization. Initially a sensitivity analysis similar to the other parameters is conducted to verify its sensitivity to the temperature and FC values. The results are presented in Fig. 11(a), revealing a minor variation attributable to changes in temperature. Interestingly, a notable difference is observed due to changes in the FC value. In the presented case, the effective change is approximately 6.3 mm, significantly higher compared to the 1.25 mm and 2.25 mm observed for previous GPI. Hence, it suggests that this parameter is more sensitive to FC and can be utilized effectively for accurately characterizing FC values in this test.

The parameter w_e value at different testing temperature is presented in the Table 3. The measured values show that at lower temperatures the w_e is higher and vice versa in contrast with the *w* that is higher at higher temperatures. This suggests a more homogeneous deformation of the sample at lower temperatures as the difference between w/w_e is smaller.

Fig. 12 presents the evolution of the ear width (w_e) against flange height (*h*) for various friction factors obtained through numerical simulation and experimental results at 1250 °C. Notably, the influence of FC on the calibration line is prominently visible this time, contributing to an overall improvement in the accuracy and a reduction in the uncertainty in the results. Specially towards the latter stages of the process, the differences become more visible, which is the desired area of interest for this analysis.

Similar to the previous case, all the repeated tests for each temperature are considered, which provides different w_e/h ratios for the FC analysis. For the inverse modelling, again various calibration lines were generated based on the simulations with different FC values. As shown in Fig. 13(a), it is evident that the experimental trials position the ratio (w_e/h) points in the region between the green and olive-coloured lines. The average FC value for this temperature (1250 °C) is estimated to be around 0.25, as indicated in the zoomed plot in Fig. 12(a).

The same methodology was employed for the tests at 1300 °C and the FC value based on the experimental data is found to between 0.2 and 0.6. Here it is visible that the experimental points are not lying on a one single calibrating curve, however by taking the average of all points, the final value of FC is estimated around 0.45, shown in the Fig. 12(b). Finally at 1360 °C, the FC increases further, the average value is estimated around 0.6. Which is a 15 % increase in the FC value compared to the previous test condition.

3.4. Effect of transfer and holding time

To streamline the process of identifying friction coefficients through inverse analysis, a state-of-the-art approach was adopted by utilizing the averaged transfer time and holding times. At 1250 °C, averaged transfer and holding times were measured to be 3.3 s and 2.54 s, respectively. Similarly, at 1300 °C and 1360 °C, the averaged transfer and holding times are 3.23 s and 3.16 s, and 2.82 s and 3.3 s, respectively. As delineated in the preceding section, to compare the experimental results with six potential friction coefficients, it is imperative to conduct six distinct T-shape numerical analyses, each corresponding to a unique friction coefficient. These individual analyses collectively contribute to the development of the master numerical curve set. Furthermore, this process needs to be iterated for each temperature under consideration. In the context of this study, this results in the creation of three numerical curve set (one per temperature), each requiring 6 T-shape numerical simulations.

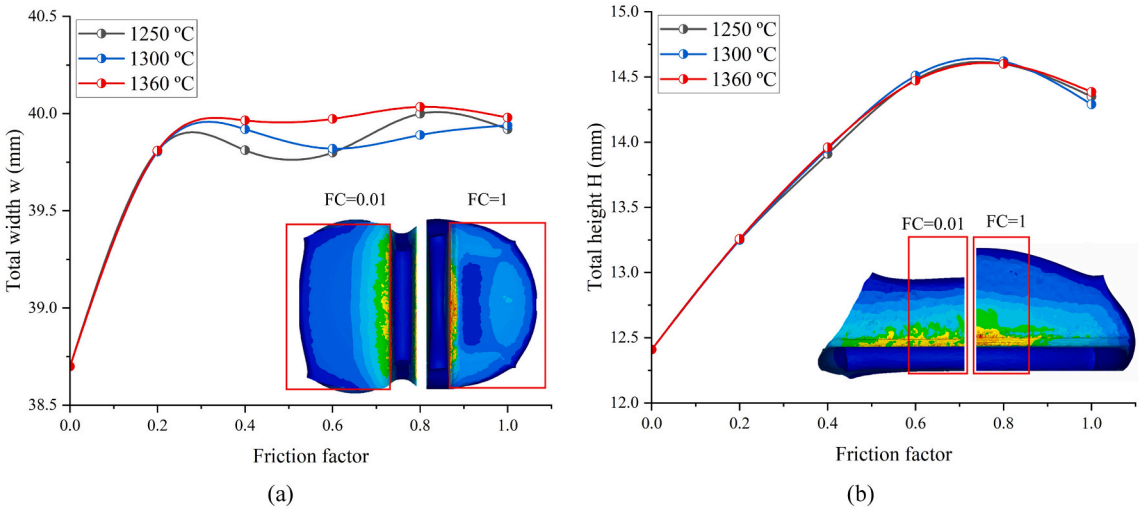

Fig. 10. Friction coefficient analysis: a) parameter total width w, b) parameter total height H.

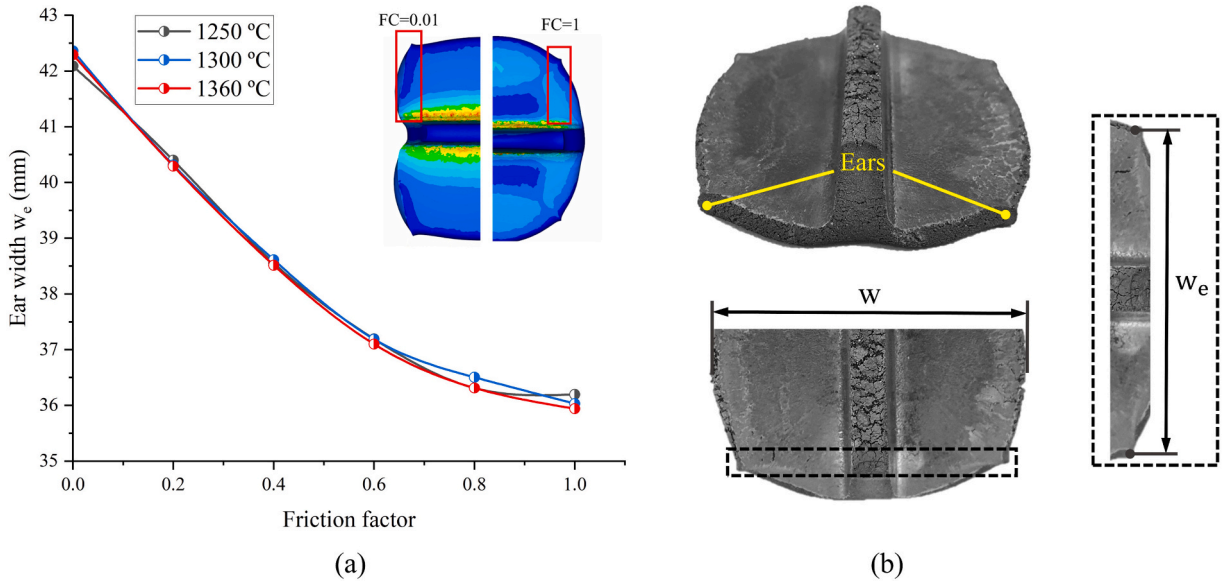

Fig. 11. New GPI index: a) sensitivity at different temperatures and friction values, b) sample measurement location.

Table 3
Test results (ears width w_e).

Temperature (°C)	1250			1300			1360		
Test no.	#1	#2	#3	#1	#2	#3	#1	#2	#3
Ears width w_e (mm)	36.7	37.6	36.4	37.2	35.4	36.2	34.5	35.8	34.5

Nonetheless, as indicated in Table 4, minor time discrepancies between tests are evident, on the order of 0.5 s for both transfer and holding times. These variations result in each billet (from the three repetitions) attaining a slightly different temperature during the forming process. Consequently, it is crucial to recognize that the averaged time hypothesis introduces an unknown error into the friction coefficient calculations. Fig. 13 visually represents the temperature differences observed from billet to billet in the experiments conducted in this study. The emissivity value of ~0.95 were considered in all tests.

In the event that precise transfer and holding times for each billet are taken into account, it implies that master numerical curve set would be valid only for the specific billet from which the data is derived. This necessitates the creation of a distinct master numerical curve set for each individual billet. As one can imagine, this significantly escalates the workload for the identification process, leading to a notable increase in the required number of T-shape numerical simulations—from 18 to 54, in this particular scenario.

To ascertain whether the additional workload is justified, an evaluation of the error introduced by the hypothesis will be conducted. For this assessment, two billets with transfer and holding times significantly deviating from the averaged values were selected. Subsequently, friction coefficient identification was executed using individual master numerical curve set for each billet. The resulting friction coefficients were then compared with the averaged value. This comparative process was executed for both the higher temperature, 1360 °C, and the lower temperature, 1250 °C. For 1250 °C test numbers #2 and #3 were used while for 1360 °C test numbers #1 and #2 were used.

Fig. 14 presents a comparison of values for the selected test samples, showcasing the contrast between employing the state-of-the-art averaged time simplification and utilizing the individual numerical curve set based on the actual real times.

Considering the marginal differences (< 5 %) observed in the obtained friction coefficients (FC), coupled with the exponential increase in workload associated with incorporating real transfer and holding times, the authors posit that the cost-benefit ratio does not warrant their inclusion. Therefore, the authors advocate for the use of averaged transfer and holding times in future studies, particularly when the variations between tests fall within the ranges demonstrated in this study.

3.5. Discussion

Based on these findings, notable variations in the friction coefficient (FC) are observed depending on the chosen geometrical parameter index (GPI). Following a sensitivity analysis of various GPIs, the authors contend that the use of the 'ear width' GPI is more appropriate for the studied conditions. Additionally, it was observed that the FC value increases with the temperature of the sample [34], indicating that material flow encounters greater resistance at higher temperatures, resulting in smaller values of ear width (see Fig. 7). Moreover, the thermal camera results showed that the cooling rate at the surface of the billet is high at higher temperatures and vice versa. Furthermore, the effect of transfer time is more noticeable on temperature compared to the holding time, which might be due to the interaction with cold air during transfer, whereas dies are kept at higher temperatures (Fig. 13).

The study reveals distinct interactions between the deformed material and dies under hot forging (1250 °C) and NSF (1360 °C) conditions. As elucidated in preceding sections, deformation inhomogeneity becomes more pronounced at elevated temperatures, as evidenced by the $w/\ w_e$ ratio. Despite established evidence indicating that transfer and holding times have minimal impact on results, it is important to recognize the existence of variables beyond friction that may contribute to the observed behaviour. Notably, the Heat Transfer Coefficient (HTC) emerges as a significant factor, as suggested by Sajjad et al. [35]. Thus, this investigation underscores the pivotal role of friction in shaping the deformation behaviour of the NSF material.

Furthermore, for a comprehensive assessment of the genuine and independent influence of friction, additional analyses should be conducted to evaluate other possible contributing factors, such as HTC under NSF conditions. Also, the authors are fully aware of the limitation of the current study which focused on a specific temperature range,

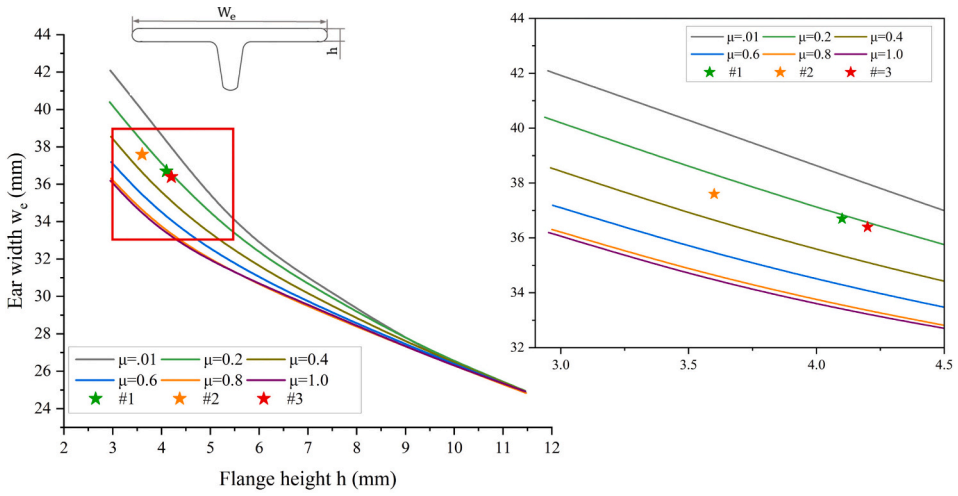

(a) 1250 °C

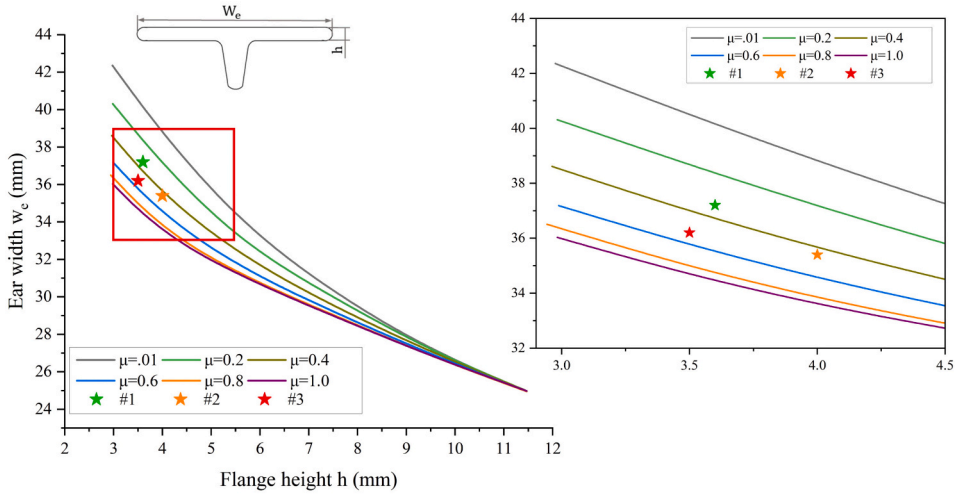

(b) 1300 °C

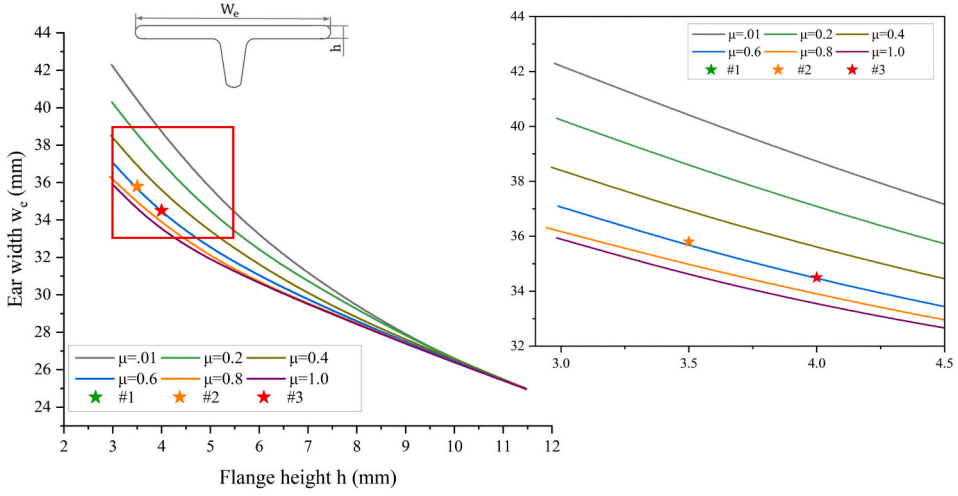

(c) 1360 °C

Fig. 12. Calibration curves and the experimental data of the T-shape test at 1250, 1300 and 1360 °C temperature.

billet dimensions and other boundary conditions. Further investigation is required to fully develop the process for vast variety of boundary conditions. Nevertheless, the proposed methodology is successfully implemented to characterize the FC at high temperatures. The new methodology is applicable to characterize the FC in majority of the deformation process employing 42CrMo4 steel at the temperatures (1250–1360 °C). In the present study the FC value of 0.25, 0.45 and 0.6 is calculated at temperature of 1250 °C, 1300 °C and 1360 °C, respectively. With all these results in hand, the authors proposed a novel calibration strategy for the friction coefficient characterization in NSF.

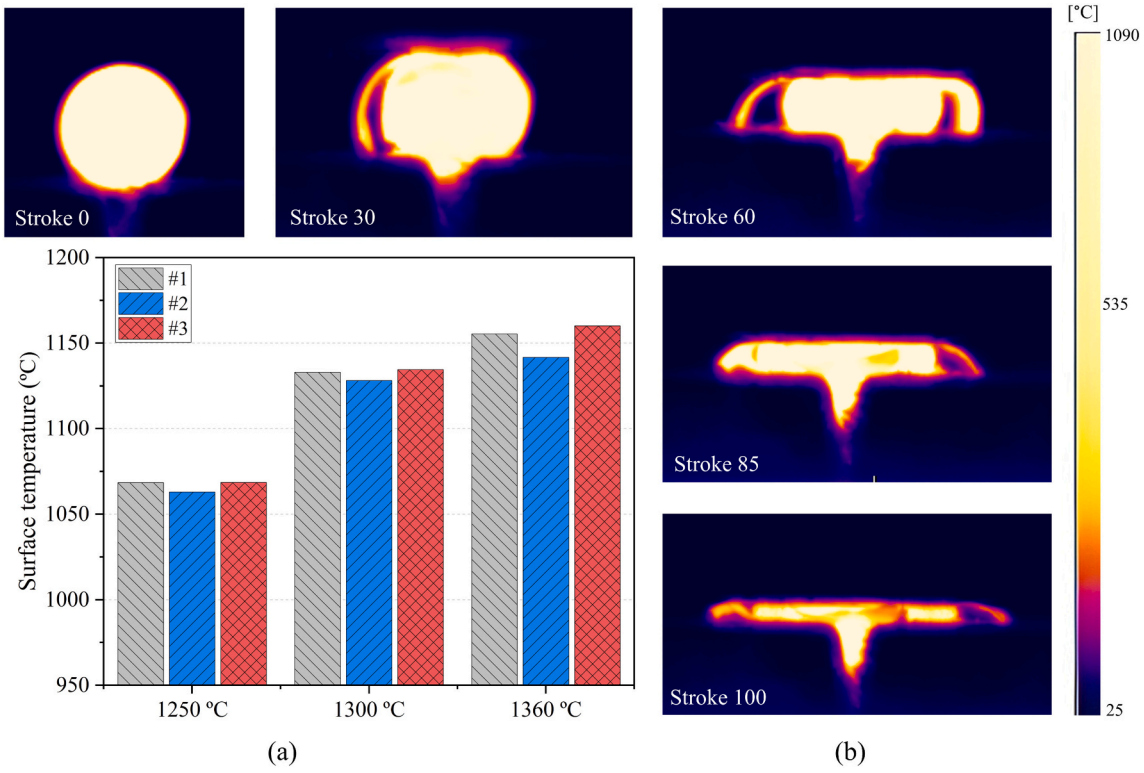

Fig. 13. Thermal camera analysis: a) surface temperature of the billet in the beginning of each test condition, b) thermal camera result at different strokes (1250 °C).

Table 4
Billet transfer and holding times in the test (experimental and singular).

Temperature (°C)	Test No.	Singular transfer time (s)	Experimental transfer time (s)	Singular holding time (s)	Experimental holding time (s)
1250	#1	3	3.2	2	2.52
–	#2	–	3.6	–	2.63
–	#3	–	3.2	–	2.48
1300	#1	–	3.1	–	3.00
–	#2	–	3.2	–	2.96
–	#3	–	3.4	–	2.52
1360	#1	–	3.0	–	3.52
–	#2	–	3.5	–	3.00
–	#3	–	3.0	–	3.48

The authors believe that the conducted study and the proposed calibration strategy will be a key factor for the future NSF material-model validation/development.

4. Conclusions

Aimed at characterizing the friction coefficient under Near Solidus Forging (NSF) conditions, the T-shape compression test was conducted on 42CrMo4 steel samples at temperatures of 1250 °C, 1300 °C, and 1360 °C. A 3D finite element model of the 42CrMo4 steel for the T-shape compression test was developed using FORGE NxT® 4.0 finite element simulation software, employing six different FC values. Results suggest that the conventional GPI, the total width and flange height introduced uncertainties in the FC estimation. Therefore, a new approach was developed to accurately characterize the FC value. Overall, the following findings were made based on the current results addressing

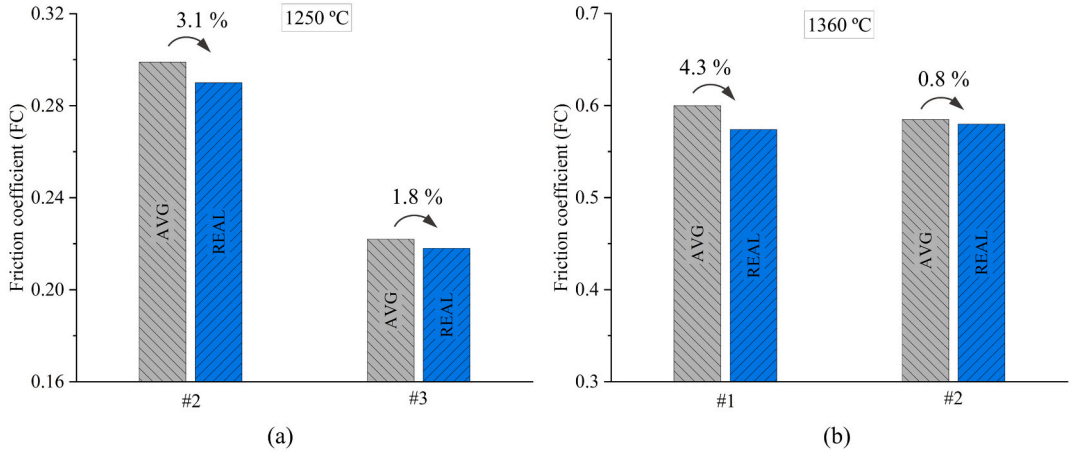

Fig. 14. Friction coefficient values at both hypotheses (average vs real; transfer and holding time).

the research gaps identified in the introduction:

- A lack of consensus in the T-Shape compression testing and inverse analysis procedure at NSF process has been characterized and solved.
- A novel geometrical parameter index based on "ear width" has been identified, as more sensitive and reliable for the friction coefficient characterization through T-shape testing under Near Solidus Forging conditions.
- As expected, in the T-shape compression test, due to thermal softening high forces are recorded at low temperatures conditions (1250 °C), whereas low force is recorded at higher temperatures (1360 °C).
- The friction coefficient was determined to be 0.25 under 1250 °C conditions, while values of 0.45 and 0.6 were observed for temperatures of 1300 °C and 1360 °C, respectively.
- The utilization of averaged transfer and holding times resulted in an error below 5 %, prompting the authors to advocate for their implementation in future studies.

With all these conclusions in hand, the authors put forth a novel calibration strategy for friction coefficient characterization under NSF conditions. The authors are confident that this study and the proposed calibration strategy will serve as pivotal information for future NSF material model calibration, which serve as a key role for the developments and industrialization of NSF process.

CRediT authorship contribution statement

Muhammad Sajjad: Writing – original draft, Visualization, Validation, Software, Methodology, Investigation, Formal analysis. **Julen Agirre:** Methodology, Investigation, Formal analysis. **Gorka Plata:** Writing – review & editing, Methodology, Investigation, Conceptualization. **Jokin Lozares:** Writing – review & editing, Methodology, Investigation, Conceptualization. **Joseba Mendiguren:** Writing – review & editing, Supervision, Resources, Project administration, Conceptualization.

Declaration of generative AI and AI-assisted technologies in the writing process

During the preparation of this work the author(s) used Chat GTP Open AI 3.5 for the re-write of the text to improve its quality. After using this tool, the author(s) reviewed and edited the content as needed and take(s) full responsibility for the content of the publication.

Declaration of competing interest

The authors declare that they have no known competing financial interests or personal relationships that could have appeared to influence the work reported in this paper.

Acknowledgments

The authors would like to acknowledge the Exploration of high entropy alloys as substitute materials for sustainable mobility and decarbonisation (HEAPLAS) project funded by Ministerio de Ciencia e Innovación, with the reference PID2022-139130OA-I00, the HSSF, Hybrid Semi-Solid Forming project funded by the "Research Fund for Coal and Steel" (RFCS) program of the European union, with the grant number 800763, and the Procesos de Fabricación de Excelentes para propiedades máximas (PROMAX), funded by Basque Government through the ELKARTEK funding scheme (reference KK-2020/00087). Also, the authors would like to thank Juan Jose Trujillo Tadeo and David Abedul Moreno for their help in the experiments.

References

[1] Lozares J, Plata G, Hurtado I, Sánchez A, Loizaga I. Near solidus forming (NSF): semi-solid steel forming at high solid content to obtain as-forged properties. Metals (Basel) 2020:10. https://doi.org/10.3390/met10020198.
[2] Plata G, Lozares J, Sánchez A, Hurtado I, Slater C. Preliminary study on the capability of the novel near solidus forming (NSF) technology to manufacture complex steel components. Materials 2020;13:1–14. https://doi.org/10.3390/ma13204682.
[3] Sajjad M, Trinidad J, Plata G, Lozares J, Mendiguren J. Sensitivity analysis of near solidus forming (NSF) process with digital twin using Taguchi approach. Adv Manuf; 2024.
[4] Bennett CJ. A comparison of material models for the numerical simulation of spike-forging of a CrMoV alloy steel. Comput Mater Sci 2013;70:114–22. https://doi.org/10.1016/j.commatsci.2013.01.003.
[5] Pierret JC, Rassili A, Vaneetveld G, Bigot R, Lecomte-Beckers J. Friction coefficients evaluation for steel thixoforging. International Journal of Material Forming 2010;3:763–6. https://doi.org/10.1007/s12289-010-0882-1.
[6] Cleary PW. Extension of SPH to predict feeding, freezing and defect creation in low pressure die casting. App Math Model 2010;34:3189–201. https://doi.org/10.1016/j.apm.2010.02.012.
[7] Fukagawa T, Okada H, Maehara Y. Mechanism of red scale defect formation in Si-added hot-rolled steel sheets. ISIJ International 1994;34:906–11. https://doi.org/10.2355/isijinternational.34.906.
[8] Zhang Q, Felder E, Bruschi S. Evaluation of friction condition in cold forging by using T-shape compression test. J Mater Process Technol 2009;209:5720–9. https://doi.org/10.1016/j.jmatprotec.2009.06.002.
[9] Deng L, Li XT, Jin JS, Wang XY, Li JJ. T-shape upsetting–extruding test for evaluating friction conditions during rib–web part forming. J Mater Process Technol 2014;214:2276–83. https://doi.org/10.1016/j.jmatprotec.2014.04.021.
[10] Sethy R, Galdos L, Mendiguren J, Sáenz de Argandoña E. Investigation of influencing factors on friction during ring test in hot forging using FEM simulation, 2016, p. 130009. doi:https://doi.org/10.1063/1.4963528.
[11] Galdos L, Saenz de Argandoña E, Mendiguren J, Sethy R, Agirre J. Characterization of Ti64 forging friction factor using ceramic coatings and different contact conditions. Procedia Eng 2017;207:2239–44. https://doi.org/10.1016/j.proeng.2017.10.988.
[12] Kim J-H, Ko B-H, Kim J-H, Lee K-H, Moon Y-H, Ko D-C. Evaluation of friction using double cup and spike forging test for dry-in-place coating and forming oils. Tribol Int 2020;150:106361. https://doi.org/10.1016/j.triboint.2020.106361.
[13] Sethy R, Galdos L, Mendiguren J, Sáenz de Argandoña E. Identification of friction coefficient in forging processes by means T-shape tests in high temperature. Key Eng Mater 2016;716:165–75. https://doi.org/10.4028/www.scientific.net/KEM.716.165.
[14] Rao KP, Xu WL. Neural evaluation of friction and flow stress adaptive to ring geometry. JSME International Journal Ser A, Mechanics and Material Engineering 1995;38:506–14. https://doi.org/10.1299/jsmea1993.38.4_506.
[15] Hoon Noh J, Ho Min K, Bok Hwang B. Deformation characteristics at contact interface in ring compression. Tribol Int 2011;44:947–55. https://doi.org/10.1016/j.triboint.2010.12.003.
[16] Buschhausen A, Weinmann K, Lee JY, Altan T. Evaluation of lubrication and friction in cold forging using a double backward-extrusion process. J Mater Process Technol 1992;33:95–108. https://doi.org/10.1016/0924-0136(92)90313-H.
[17] Arentoft M, VC, LM, & BN. A study of the double cup extrusion process as a friction test. In Proceed. of the 5th Int. Conf. on Technol. of Plasticity, 1996, p. 243–50.
[18] Schrader T, Shirgaokar M, Altan T. A critical evaluation of the double cup extrusion test for selection of cold forging lubricants. J Mater Process Technol 2007;189:36–44. https://doi.org/10.1016/j.jmatprotec.2006.11.229.
[19] Xu WL, Rao KP. Analysis of the deformation characteristics of spike-forging process through FE simulations and experiments. J Mater Process Technol 1997;70:122–8. https://doi.org/10.1016/S0924-0136(97)00048-4.
[20] Hu C, Ou H, Zhao Z. Investigation of tribological condition in cold forging using an optimized design of spike forging test. Adv Mech Eng 2015;7:168781401558721. https://doi.org/10.1177/1687814015587212.
[21] Fereshteh-Saniee F, Badnava H, Pezeshki-Najafabadi SM. Application of T-shape friction test for AZ31 and AZ80 magnesium alloys at elevated temperatures. Mater Des 2011;32:3221–30. https://doi.org/10.1016/j.matdes.2011.02.042.
[22] Sethy R, Galdos L, Mendiguren J, Sáenz de Argandoña E. Friction and heat transfer coefficient determination of titanium alloys during hot forging conditions. Adv Eng Mater 2017:19. https://doi.org/10.1002/adem.201600060.
[23] Yan X, Zhang S, Huang K, Yang Y, Wang W, Wu M. Effect of holding time on the extrusion force and microstructure evolution during the plastic forming of Ti-6Al-4V Micro-gears. Materials 2022;15:1507. https://doi.org/10.3390/ma15041507.
[24] Rooks BW, Singh AK, Tobias SA. Temperature effects in hot forging dies. Metals Technology 1974;1:449–55. https://doi.org/10.1179/030716974803287799.
[25] Xiao G, Jiang J, Wang Y, Liu Y, Zhang Y. Effects of forming temperature, soaking time and dwell time on the microstructure and mechanical properties of thixoformed nickel-based superalloy parts. J Mater Res Technol 2021;10:1250–61. https://doi.org/10.1016/j.jmrt.2020.12.111.
[26] Barati F, Nemati Y. Application of T-shape friction T test for Ti-6Al-4V alloy at elevated temperatures. Journal of Simulation and Analysis of Novel Technologies in Mechanical Engineering 2014;7:53–62.
[27] Yoon JH, Lee SI, Jeon HW, Lee JH. Study on the lubrication characteristics at the elevated temperature in hot forging test with extruded AZ80 mg alloy. Transactions of Materials Processing 2013;22:108–13. https://doi.org/10.5228/KSTP.2013.22.2.108.

[28] Liu Q, Li W, Zhu L, Gao Y, Xing L, Duan Y, et al. Temperature-dependent friction coefficient and its effect on modeling friction stir welding for aluminum alloys. J Manuf Process 2022;84:1054–63. https://doi.org/10.1016/j.jmapro.2022.10.068.
[29] Meyghani B. A modified friction model and its application in finite-element analysis of friction stir welding process. J Manuf Process 2021;72:29–47. https://doi.org/10.1016/j.jmapro.2021.10.008.
[30] Dialami N, Chiumenti M, Cervera M, Segatori A, Osikowicz W. Enhanced friction model for friction stir welding (FSW) analysis: simulation and experimental validation. Int J Mech Sci 2017;133:555–67. https://doi.org/10.1016/j.ijmecsci.2017.09.022.
[31] Jiang H, Yan G, Li J, Xu J, Shan D, Guo B. Deformation behavior and microstructural evolution of T-shape upsetting test in ultrafine-grained pure copper. Materials 2021;14:4869. https://doi.org/10.3390/ma14174869.
[32] Bilbao O, Loizaga I, Alonso J, Girot F, Torregaray A. 42CrMo4 steel flow behavior characterization for high temperature closed dies hot forging in automotive components applications. Heliyon 2023;9:e22256. https://doi.org/10.1016/j.heliyon.2023.e22256.
[33] Becker E, Bigot R, Rivoirard S, Faverolle P. Experimental investigation of the thixoforging of tubes of low-carbon steel. J Mater Process Technol 2018;252:485–97. https://doi.org/10.1016/j.jmatprotec.2017.10.003.
[34] Rudkins NT, Hartley P, Pillinger I, Petty D. Friction modelling and experimental observations in hot ring compression tests. J Mater Process Technol 1996;60:349–53. https://doi.org/10.1016/0924-0136(96)02353-9.
[35] Sajjad M, Plata G, Lozares J, Mendiguren J. Digital twin development for the sensitivity analysis of near solidus forming process. Materials Research Proceedings 2023;28:1521–30. https://doi.org/10.21741/9781644902479-164.